ARTICLE NO. 78-1129R

Boundary-Layer Transition Experiments on Sharp, Slender Cones in Supersonic Free Flight

Daniel C. Reda*
Naval Surface Weapons Center, White Oak Laboratory, Silver Spring, Md.

Transition experiments were conducted on sharp, slender ($\theta_c = 5$ deg) cones at $M_\infty = 4.5$ in an aeroballistics range. Data acquisition was accomplished with dual-plane spark shadowgraphs. Wall-to-adiabatic wall temperature ratio was varied from $\simeq 0.2$ to $\simeq 0.5$ by cryogenically cooling the range gas at two distinct edge unit Reynolds numbers, $(U_e/\nu_e) = 0.37$ and 1.11×10^6/cm (0.94 and 2.82×10^6/in.). Unit Reynolds number influence on transition and transition zone asymmetry (TZA) as a function of nondimensional angle of attack (α/θ_c) were also investigated. Transition reversals with increased wall cooling were noted at both (U_e/ν_e) values. A strong unit Reynolds number influence on transition was observed for $(U_e/\nu_e) > \simeq 3.94 \times 10^5$/cm ($10^6$/in.), substantiating results of Potter. Comparisons of present TZA data with the empirical model of Potter and with other $M_\infty \simeq 5$ data showed that transition contours, at $(\alpha/\theta_c) > 0$, may not be adequately described by a singular dependence on (α/θ_c).

Nomenclature

C = speed of sound
M = Mach number
n = exponent of unit Reynolds number
p = pressure
$\tilde{p}$ = fluctuating pressure
Re_{TR} = transition Reynolds number, $\rho_e U_e X_{TR}/\mu_e$
r = recovery factor
T = temperature
U = velocity
X_{TR} = transition run length
α = angle of attack
γ = ratio of specific heats
θ_c = cone half-angle
μ = viscosity
ν = kinematic viscosity
ρ = density
ϕ = circumferential angle, measured from windward ray

Subscripts

aw = adiabatic wall
e = at edge of boundary layer, or based on edge properties
w = at wall, or based on wall properties
$\alpha = 0$ = at zero angle of attack
∞ = freestream

Introduction

BOUNDARY-LAYER transition, aside from being one of the classical unsolved problems of basic fluid physics, remains a real-world problem to designers of advanced flight systems. Accurate predictions of viscous flowfields around high-speed aircraft, missiles, and re-entry vehicles are of paramount importance to each system's design and subsequent flight performance. Boundary-layer transition is known to affect vehicle dynamics, drag, and surface heat-transfer rates significantly. To date, universally valid empirical and/or semiempirical correlations for boundary-layer transition onset, location, and degree of symmetry (or asymmetry), as a function of one or more of the many variables which influence it, have been lacking. The great reservoir of experimental data obtained under wind tunnel conditions has recently come under critical scrutiny due to findings which demonstrated that facility noise can dominate or seriously compromise transition results.[1,2] These facts, and many other pertinent, unanswered questions concerning this phenomenon, have been documented in the detailed surveys of Morkovin[3,4] and Reshotko.[5]

Due to the critical nature of this problem area, there evolved at the beginning of the present decade a national committee, the U.S. Transition Study Group (USTSG). Its objectives were "to develop and implement a program that would do something constructive toward resolving the many observed anomalies in boundary-layer transition data and that might provide some basis for future estimation of transition Reynolds numbers. The group formulated specific experimental programs emphasizing careful and redundant measurements, documentation of the disturbance environment, and elimination, wherever possible, of facility induced transition." Dr. Eli Reshotko of Case Western Reserve University was named Chairman; his recent paper[6] summarizes the Committee's recommended research program.

The "pre-committee" research of Sheetz[7,8] at the Naval Ordnance Laboratory, and of Potter[9] at the Arnold Engineering and Development Center (AEDC), had demonstrated the utility of ballistics ranges for boundary-layer transition research. This capability for conducting transition experiments in quiescent environments resulted in the Committee's formulation of additional research tasks to be conducted at both laboratories.[6]

The AEDC was to focus on unit Reynolds number effects, while also conducting a series of sensitivity studies on various test-related factors that might influence transition in ballistics-range environments. This research was conducted by Potter and reported in Refs. 10 and 11.

The objective of this research was to investigate experimentally the influence of wall-to-adiabatic wall temperature ratio on smooth-wall boundary-layer transition in supersonic free flight. In addition to this primary objective,

Received July 5, 1978; presented as Paper 78-1129 at the AIAA 11th Fluid and Plasma Dynamics Conference, Seattle, Wash., July 10-12, 1978; revision received May 1, 1979.

Index categories: Boundary-Layer Stability and Transition; Supersonic and Hypersonic Flow.

*Currently Member, Technical Staff, Aerodynamics Dept., Sandia Laboratories, Albuquerque, N. Mex. Associate Fellow AIAA.

an independent check on the unit Reynolds number phenomenon, as observed by Potter in the AEDC ballistic range, was to be made. Experimental results concerning both these questions were obtained, along with information concerning boundary-layer transition zone asymmetry due to small angles of attack. These results are presented herein as the Naval Ordnance Laboratory's contribution to the USTSG's research program.

II. Definition of Test Environments

Inviscid calculations were undertaken in order to define free flight test environments wherein $(T_w/T_{aw})_e$ could be varied over a finite regime as the independent variable, while holding both M_e and (U_e/ν_e) fixed. A sharp, slender ($\theta_c = 5$ deg) cone geometry was selected as consistent with the nature of USTSG objectives and compatible with testing in a ballistics range facility.

For the short flight times encountered in such facilities, cone surface temperature (T_w) remains essentially constant at its initial value $\simeq 300$ K ($\simeq 540°$R), except in the immediate vicinity of the cone tip. Variations in $(T_w/T_{aw})_e$ are thus accomplished through variations in the recovery, or adiabatic-wall, temperature of the flow. For a sharp cone at zero incidence:

$$(T_{aw})_e = T_e\left[1 + r\left(\frac{\gamma-1}{2}\right)M_e^2\right] \tag{1}$$

where $r = $ const. (here 0.9) and

$$\frac{T_e}{T_\infty} = \left[1 + \left(\frac{\gamma-1}{2}\right)M_\infty^2\right] \Big/ \left[1 + \left(\frac{\gamma-1}{2}\right)M_e^2\right] \tag{2}$$

Thus, for a given cone geometry at a given M_∞, $(T_{aw})_e$ varies in direct proportion to T_∞, the static temperature of the range gas.

A test technique was thereby defined wherein T_∞ would be independently varied to achieve the desired variations in $(T_w/T_{aw})_e$. In order to insure a constant flight Mach number, cone launch velocity would be properly chosen to match each T_∞ level ($M_\infty = U_\infty/C_\infty$ with $C_\infty \propto \sqrt{T_\infty}$). Further P_∞ would be independently set for each flight to insure a constant edge unit Reynolds number (U_e/ν_e). Figures 1 and 2 show results of such calculations in the regime $0.2 \leq (T_w/T_{aw})_e \leq 0.6$ for a 5 deg half-angle cone at $M_\infty = 4.5$ ($M_e = 4.27$), for $(U_e/\nu_e) = 3.67$ and 11.64×10^5/cm (9.33 and 29.56×10^5/in.), for flights in nitrogen.

Secondary test objectives were to be met by conducting a series of $M_\infty = 4.5$ flights at room temperature conditions, $(T_w/T_{aw})_e = 0.21$, with variations in (U_e/ν_e) being accomplished through variations in freestream static pressure.

III. Experimental Apparatus

A brief summary of experimental apparatus and test procedures is given below. A more detailed discussion of these topics, and a complete tabulation of all results, are given in the original preprint and in Ref. 12.

All models were launched without spin from a single-stage, powder-driven, smooth-bore gun, 4.128 cm (1.625 in.) I.D. The model/sabot package, shown in Fig. 3, incorporated the hollow-base/bore-size model design used by Potter.[10,11]

After traversing a flight distance of 44.58 m (146.25 ft) from the muzzle, the model entered an environmental chamber, where primary data acquisition occurred. Within this chamber various uniform-temperature-level environments of gas were established prior to launch via cryogenic cooling.

Three pairs of spark-source/single-pass shadowgraphs were used to optically record flowfields about the free-flight models within the chamber. Each pair was arranged in a dual-plane mode so as to provide simultaneous perpendicular views of the model. Spark firing times were 0.2 μs in duration.

Noise measurements made within the chamber yielded results essentially identical to rms levels reported by Potter,[10,11] $(\bar{p}/p_\infty)_{max} = 2.1$ to 2.8×10^{-6}. Such levels are three to four orders of magnitude below those associated with wind-tunnel facilities.[13]

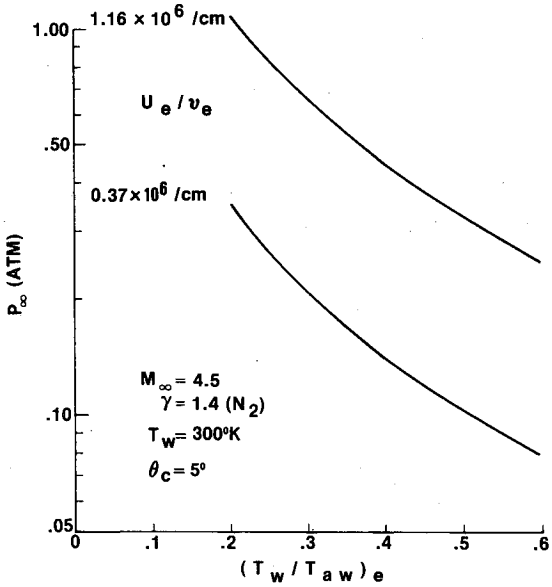

Fig. 2 Definition of test conditions—pressure.

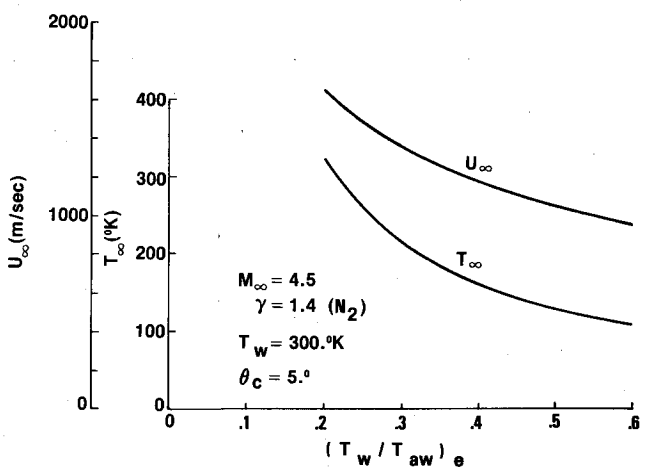

Fig. 1 Definition of test conditions—velocity and temperature.

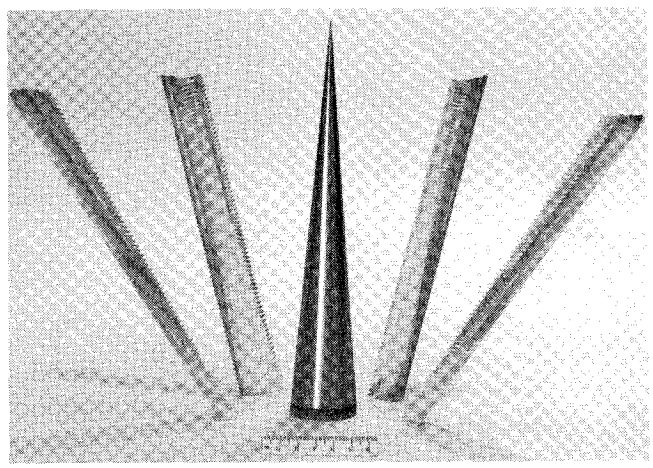

Fig. 3 Photograph of model and sabot.

Other experimental factors of concern are summarized below; more extensive discussions of these issues are also given in Ref. 12.

Each model was fabricated from an integral piece of titanium, and thus possessed no surface discontinuities. Maximum surface roughness values ranged from 0.147 to 0.211 μm (5.8 to 8.3 μ in.), rms, or 0.584 to 0.838 μm (23 to 33 μ in.), peak to valley.† Surface waviness was measured at 1.52 to 4.57×10^{-4} cm (0.6 to 1.8×10^{-4} in.) maximum amplitude, peak to valley, with wavelengths ranging from 0.56 to 0.89 cm (0.22 to 0.35 in.), peak to peak.

Recovery temperatures associated with present test environments were always below titanium melt levels. A model nosetip radius of 0.0127 cm (.005 in.) was selected to insure complete entropy swallowing within the initial 2.54 cm (1.0 in.) of wetted length measured from the stagnation point; measured run lengths to transition were $\geq$6.35 cm (2.5 in.) and thus all data were obtained in the sharp-cone regime.

IV. Data Reduction Procedures

Transition location X_{TR} was defined (and read) as that run length along each conical ray to the station where breakdown to turbulence was complete; i.e., downstream of this location, no further regions of intermittent laminar flow were observed. This definition of X_{TR} corresponds to locations near the middle to end of a transition zone as defined by conventional surface heat-transfer and/or surface pitot-probe techniques.[14] It should be further noted that shadowgraphs provide an instantaneous record of a basically unsteady flow phenomenon and that a distribution of X_{TR} values is expected, even for nominally steady-flow conditons (e.g., Fig. 3 of Ref. 14).

Perpendicular views of the model silhouette at each station allow the total model angle-of-attack, the plane in which it occurs, and the circumferential orientation of each photographed ray relative to the true windward ray to be determined.[15] A primary ray is thus defined as the ray closest to true windward ($\phi<45$ deg).

Having defined an X_{TR} value on the primary ray, it remains to correct this measured value for angle-of-attack effects. Figure 4 presents the set of curves used by Potter[10,11] for this purpose. These curves give a description of transition-zone asymmetry on sharp, slender cones as a function of nondimensional angle of attack (α/θ_c) and are based on transition zone location data, measured via shadowgraph and/or surface heat-transfer techniques, in the wind tunnel experiments of Ward,[16] DiCristina,[17] and Mateer.[18] Implicit in this figure is the assumption that, while noise, unit Reynolds number, wall-temperature ratio, etc., influence transition zone location on a cone at zero incidence, once this run length ($X_{TR,\alpha=0}$) is determined for any particular set of test conditions, then the development of transition zone asymmetry with increasing angle of attack is solely a function of (α/θ_c). As noted in Fig. 4, corrections to present primary-ray data ($\phi<45$ deg) for $\phi>0$ deg, $\alpha>0$ deg were obtained by linear interpolation between the $\phi=0$ and $\phi=60$ deg curves, $0\leq(\alpha/\theta_c)\leq0.6$, and, as a result, were generally small. (Sensitivity of present results to the correction procedure used will be discussed in Section V.C.)

V. Results

A. Wall Temperature Ratio Results

Effects of wall cooling on stability and transition of compressible laminar boundary layers have been investigated in a significant number of wind tunnel experiments, with widely varying results being documented.

†For present test conditions, roughness Reynolds numbers calculated using the stated maximum roughness height, and conditions in the laminar boundary layer at this height, were found to be $\leq$4.0 for X $\geq$ 1.25 cm.

Based on theoretical work of Refs. 19-21, Reshotko[22] discussed effects of wall cooling on the stabilization of first- and second-mode disturbances. He noted, in concurrence with Ref. 23, that observed differences in transition behavior with wall cooling could not be explained by differing measurement techniques, but rather were a result of differing dominating frequencies in the disturbance spectra associated with the various facilities utilized. Further, depending on the (U_e^2/ν_e) regime, variations in $(T_w/T_{aw})_e$ could have a differing influence on stabilization of the various disturbance modes; the higher the value of (U_e^2/ν_e), the less the importance of the higher modes and the more likely that a given disturbance frequency would correspond to the lowest mode. Transition reversals with increased cooling could thus be reasonably expected based on linear stability arguments.

The only controlled, ground-based experiments into wall-cooling effects on transition, in the absence of radiated noise and freestream turbulence, are those ballistics range experiments of Sheetz[7] and the present effort. Such free-flight experiments have an advantage associated with data acquisition in truly quiescent environments. However, by their very nature, barring significant breakthroughs in physical integrity and cost of telemetry-type instrumentation, such experiments are limited to macroscopic observations of the phenomenon in question. The exact nature of transition-promoting disturbances and how they are amplified by the laminar boundary layer, leading to its eventual breakdown to turbulence, cannot be ascertained from range testing alone. Detailed microscopic experiments such as those conducted by Kendall[24] are a necessary complement to this work, as called for in the USTSG recommended program for transition research.[6]

Figure 5 shows a plot of transition Reynolds number vs wall to adiabatic wall temperature ratio, for each of two distinct edge unit Reynolds numbers, as measured during the present experiment. At high unit Reynolds number 1.10×10^6/cm (2.8×10^6/in.), transition data were obtained over the $(T_w/T_{aw})_e$ regime from 0.51 to 0.23; cooling was noted to be destabilizing from 0.51 to $\simeq$0.35, and stabilizing from $\simeq$0.35 to 0.23. At low unit Reynolds number 0.37×10^6/cm (0.94×10^6/in.), transition data were obtained over a slightly less expanded $(T_w/T_{aw})_e$ regime, from 0.45 to 0.22; here, no established trend was noted with cooling from 0.45 to 0.3, whereas a definite stabilizing influence was evident from $\simeq$0.3 to 0.22, just as in the higher unit Reynolds number case.

A destabilizing influence (decreasing Re_{TR}), followed by a stabilizing influence (increasing Re_{TR}), is here referred to as a "transition reversal." If one speculates on the functional

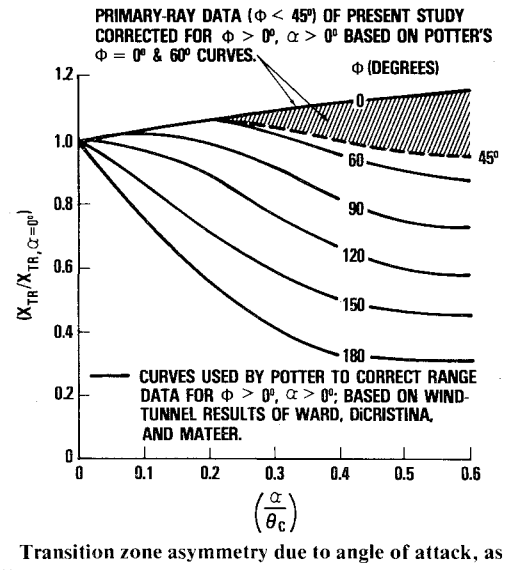

Fig. 4 Transition zone asymmetry due to angle of attack, as reported by Potter.

SYM.	θ_c	M_∞	M_e	U_e/ν_e, 1/cm	U_e^2/ν_e, 1/SEC.	FACILITY
△	5°	4.4	4.2	1.11×10^8	$1.04 - 1.66 \times 10^{11}$	RANGE
○		4.5	4.3	0.37×10^8	$0.39 - 0.53 \times 10^{11}$	

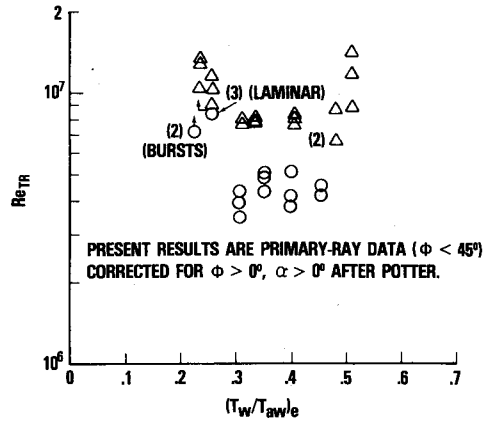

Fig. 5 Transition Reynolds number vs. wall-to-adiabatic wall temperature ratio—present data.

SOURCE	SYM.	θ_c	M_∞	M_e	U_e/ν_e, 1/cm.	U_e^2/ν_e, 1/SEC.	FACILITY
REDA	△	5°	4.4	4.2	1.11×10^8	$1.04 - 1.66 \times 10^{11}$	RANGE
	○		4.5	4.3	0.37×10^8	$0.39 - 0.53 \times 10^{11}$	
POTTER	▨	10°	5.0	4.3	$\sim 1.18 \times 10^8$ $\sim 0.31 \times 10^8$	$\sim 2.0 \times 10^{11}$ $\sim 0.53 \times 10^{11}$	RANGE
	▤	10°	2.3	2.1	$\sim 1.18 \times 10^8$ $\sim 0.35 \times 10^8$	$\sim 0.90 \times 10^{11}$ $\sim 0.27 \times 10^{11}$	
SHEETZ	◇	5°	4.9	4.6	$\sim 0.87 \times 10^8$	$1.3 - 2.9 \times 10^{11}$	RANGE

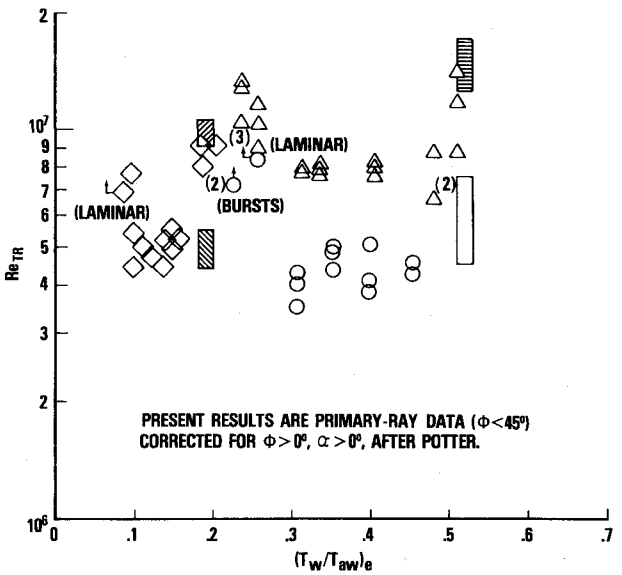

Fig. 6 Transition Reynolds number vs wall-to-adiabatic wall temperature ratio—present data vs Potter and Sheetz.

dependence of Re_{TR} on $(T_w/T_{aw})_e$ from 1.0 to $\simeq 0.5$ (the maximum value of the present experiment), based, say, on results of Ref. 25, then this observed behavior might also be referred to as a "transition re-reversal." The potential for multiple-reversals must be acknowledged, based on the gun-tunnel/flat-plate transition results of Richards and Stollery[23] and the shock-tube/wall-boundary-layer transition studies of Boison.[26]

Reversals in Re_{TR} with cooling also tend to discount further any plausible arguments concerning surface roughness effects on transition under present test conditions; since the laminar boundary layer tends to thin with increased cooling, surface

SOURCE	SYM.	θ_c	M_∞	M_e	U_e/ν_e, 1/cm.	U_e^2/ν_e, 1/SEC.	FACILITY
REDA	△	5°	4.4	4.2	1.11×10^8	$1.04 - 1.66 \times 10^{11}$	RANGE
	○		4.5	4.3	0.37×10^8	$0.39 - 0.53 \times 10^{11}$	
STETSON	◇	8°	5.5	4.9	$0.07 - 0.19 \times 10^8$	$0.09 - 0.29 \times 10^{11}$	SHOCK TUNNEL
KROGMANN	----	5°	5.0	4.7	0.18×10^8 $0.13 - 0.31 \times 10^8$	$0.13 - 0.18 \times 10^{11}$ $0.13 - 0.25 \times 10^{11}$	LUDWIEG TUBE

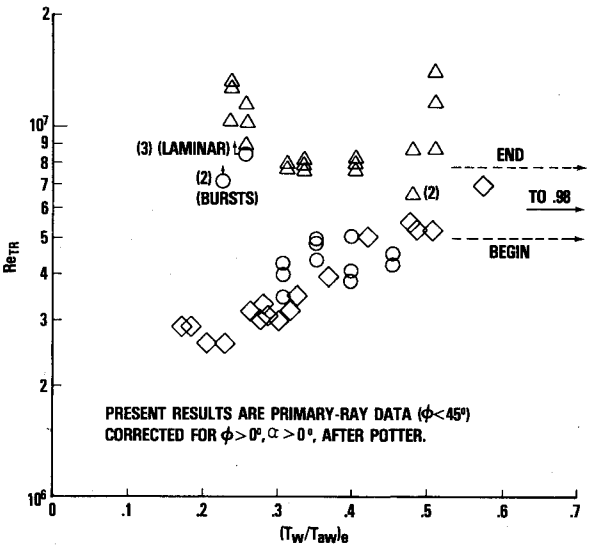

Fig. 7 Transition Reynolds number vs wall-to-adiabatic wall temperature ratio—present data vs Stetson and Krogmann.

roughness, if a dominant factor, would tend to further decrease observed transition Reynolds numbers, counter to observed behavior.

Figures 6 and 7 show comparisons of present results with data from four other sources: Potter,[10,11] Sheetz,[7] Stetson,[27] and Krogmann.[28] In all cases, transition measurements were made on sharp, slender cones in the edge Mach number regime from four to five.

In Fig. 6, comparisons are made solely with other ballistics range data. Sheetz[7] varied the wall temperature ratio by use of an environmental chamber, employing a test procedure similar to the one used here; in Ref. 7, data at $(T_w/T_{aw})_e < 0.2$ for $M_\infty \simeq 5$ were obtained by heating the volume of test gas above room temperature. Potter's[10,11] two values of $(T_w/T_{aw})_e$ resulted solely from the fact that tests were conducted at two different Mach numbers, with $T_\infty \cong 300$ K (540°R). Two points are noted here. First, Potter's $M_e = 4.3$ and 2.1 data are seen to be in nominal agreement with transition Reynolds numbers measured here. The collapse of his two separate Mach number data sets in transition Reynolds number vs unit Reynolds number coordinates may be because these data sets apparently bracket a region of transition reversal. Second, Sheetz's observation of a transition reversal at colder wall conditions than those of the present experiment represents another demonstration of the potential for multiple reversals of Re_{TR} with wall cooling (recall Refs. 23 and 26).

In Fig. 7, comparisons are made with two data sets obtained in facilities other than conventional wind tunnels: the shock tunnel results of Stetson[27] and the Ludwieg tube results of Krogmann.[28] Wall temperature ratio variations were accomplished, in the first case, through variations in shock strength and, in the second case, through variations in reservoir total temperature. These data sets provide interesting comparisons for two reasons. First, maximum (U_e/ν_e) and (U_e^2/ν_e) values for these experiments are of the same order as minimum values experienced in the present effort. Second, although not documented, disturbance environments associated with these two facility types may be

significantly different from those experienced in conventional/long-run-time wind tunnels (along these lines, no unit-Reynolds-number influence on transition was observed in either facility, as will be illustrated in the next subsection).

Krogmann[28] found no dependence of Re_{TR} on wall cooling in the regime $0.98 \geq (T_w/T_{aw})_e \geq 0.5$. Stetson's data[27] showed a definite destabilizing influence (decreasing Re_{TR}) as $(T_w/T_{aw})_e$ was varied from $\simeq 0.5$ to $\simeq 0.2$, at which point a slight indication of a stabilizing influence (or possible reversal) was noted. Considering the nearly identical M_e, (U_e/ν_e) and (U_e^2/ν_e) values of these two experiments, it is perhaps more than coincidental that the resulting data sets merge, in good agreement with one another, at their point of overlap $(T_w/T_{aw})_e \simeq 0.5$.

Transition Reynolds numbers measured at low (U_e/ν_e) in the present experiment were noted to be in good quantitative agreement with values measured by Stetson, in the wall temperature ratio regime $\simeq 0.45$ to $\simeq 0.3$. Trends with increased cooling, however, were noted to be somewhat different, with a transition reversal clearly indicated at $(T_w/T_{aw})_e \simeq 0.3$ in the present case vs a possible reversal at $\simeq 0.2$ in the Stetson experiment.

B. Unit Reynolds Number Effects

Technical background concerning this most perplexing issue is well summarized in the discussions of Reshotko[5,22] and the most recent reviews of Whitfield and Dougherty[29] and Morkovin.[3,4] Reshotko[5,22] presented a mathematical argument based on dimensional analysis and linear stability theory which dictates a power-law dependence between transition Reynolds number and either a nondimensional frequency proportional to (U_e^2/ν_e) or a nondimensional wavelength proportional to (U_e/ν_e), depending on whether the disturbance spectrum is best characterized by a physical frequency or wavelength. Whitfield and Dougherty,[29] reiterating and extending the work of Pate and Schueler,[1] further demonstrated that acoustic disturbances radiated by turbulent wall boundary layers play a dominant role in boundary-layer transition as measured in wind tunnel facilities. Since such disturbances scale with unit Reynolds number, at least a partial explanation for this phenomenon as observed in wind tunnel experiments has been afforded. Morkovin[3,4] has stated that the unit Reynolds number effect on transition is more likely attributable to a combined response of the laminar boundary layer to a superposition of several or more (usually unknown) disturbance factors; a single, unique dependence of transition Reynolds number on unit Reynolds number should not, therefore, be expected.

Figure 8 shows a plot of transition Reynolds number vs unit Reynolds number; present data are shown in comparison with the ballistics range data of Potter[10,11] and Sheetz.[7] Except for the addition of Potter's Mach 2 data, all results were obtained for $M_e \simeq 4.5$ and $(T_w/T_{aw})_e \simeq 0.2$. In all cases, unit Reynolds number variations were obtained through variations in the freestream static pressure level at constant freestream velocity and static temperature. The dimensional frequency (U_e^2/ν_e) thus varied proportionately with unit Reynolds number.

Within the unit Reynolds number range $\simeq 0.59$ to $\simeq 1.18 \times 10^6$/cm. ($\simeq 1.5$ to $\simeq 3.0 \times 10^6$/in.), present data were found to support the strong unit Reynolds number influence on transition observed by Potter. A least-squares fit of present results in this stated regime for Re_{TR} proportional to $(U_e/\nu_e)^n$ yielded a value for the exponent n of 0.71, approximately 10% above the 0.63 value dictated by the combined data sets of Potter. Since all unit Reynolds number tests were conducted at room temperature, supplemental shadowgraph pictures were also obtained from the split-beam stations within the range tube itself; these data, although not plotted with the primary-ray data of Fig. 8, further confirmed the stated 0.71 value.

SOURCE	SYM.	θ_c	M_∞	M_e	$(T_w/T_{aw})_e$	U_e^2/ν_e, 1/SEC.	FACILITY
REDA	○	5°	4.4	4.2	.22	.28 - 1.66 x 10^{11}	RANGE
POTTER	– –	10°	5.0	4.3	.19	.42 - 5.27 x 10^{11}	RANGE
	– –	10°	2.3	2.1	.52	.17 - 1.00 x 10^{11}	RANGE
SHEETZ	□	5°	5.0	4.8	.19	1.40 - 1.71 x 10^{11}	RANGE

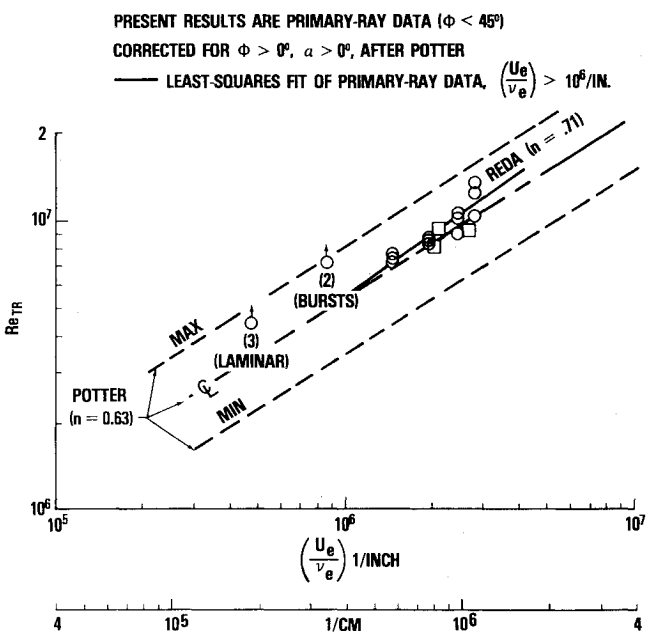

Fig. 8 Transition Reynolds number vs unit Reynolds number—present data vs Potter and Sheetz.

Transition Reynolds numbers measured on those two flights at unit Reynolds numbers below 0.39×10^6/cm(10^6/in.) were noted to be less consistent with Potter's data. During the higher unit Reynolds number test of these two, transition was complete only on the leeward side; indications of turbulent bursts were clearly evident on the primary ray, but they occurred too near the end of the test surface to allow a conclusive statement concerning complete breakdown to turbulence. The lowest unit Reynolds number flight was completely laminar on all rays, with transition being observed in the recompression region of the near wake. Therefore, while no decisive statement can be made concerning unit Reynolds number influence on transition in this regime, these data, when viewed vs an extension of the least-squares-fit to data above 0.39×10^6/cm (10^6/in.), appear to indicate a lessening (U_e/ν_e) influence on Re_{TR} as unit Reynolds number is decreased.

Transition Reynolds numbers measured at high and low unit Reynolds numbers, as plotted in Fig. 5, were paired at nominal wall temperature ratio values of 0.30, 0.35, 0.40, and 0.45 and plotted in Re_{TR} vs (U_e/ν_e) coordinates. The so-called unit Reynolds number effect was seen to persist; while no systematic dependency of the exponent n on $(T_w/T_{aw})_e$ was noted, its value remained in the 0.4-0.7 regime.

Figure 8 also shows transition Reynolds numbers measured by Sheetz[7] at $(T_w/T_{aw})_e \simeq 0.2$, as replotted from Fig. 6. His data were noted to be in close quantitative agreement with both present data and Potter's results, but were too limited in scope to define any trend with unit Reynolds number at stated test conditions. Sheetz[8] did, however, conduct a limited test series wherein (U_e/ν_e) was the primary independent variable; results obtained on sharp slender cones at $M_e \simeq 7$ for $\simeq 0.39 \times 10^6 \leq (U_e/\nu_e) \leq \simeq 0.39 \times 10^7$/cm ($\simeq 10^6 \leq (U_e/\nu_e) \leq \simeq 10^7$/in.) defined an exponent $n \simeq 0.21$. This finding, when viewed in combination with the $M_e \simeq 4.5$ results, illustrates a potential Mach number influence on the phenomenon in question.

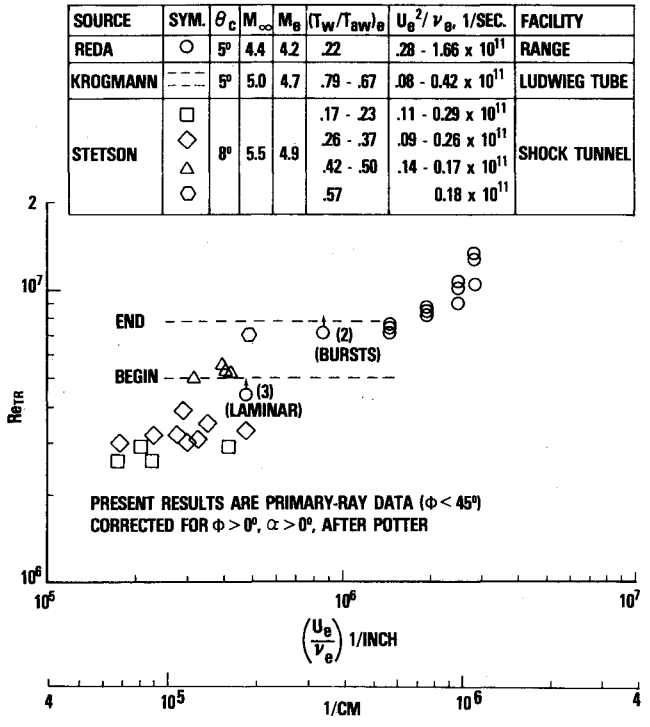

Fig. 9 Transition Reynolds number vs unit Reynolds number—present data vs Krogmann and Stetson.

In summary, combined ballistics range results have shown a unit Reynolds number influence on transition of equal or greater magnitude than found in wind tunnel experiments. Further, the physical mechanism(s) for this influence, for flights through quiescent environments, has yet to be defined.

Figure 9 shows a comparison of present unit Reynolds number data with results of Stetson[27] and Krogmann.[28] In Stetson's experiment, unit Reynolds number variations resulted from variations in initial shock-tube static pressure and shock strength; in Krogmann's experiment, they resulted from variations in the reservoir stagnation pressure.

Krogmann observed no unit Reynolds number influence on transition over the wall temperature ratio regime 0.67 to 0.79. Similarly, if one subdivides Stetson's data into discrete sets, with $(T_w/T_{aw})_e \simeq$ const. as was done in Fig. 9, then the absence of any unit Reynolds number influence on transition in his experiment is also clearly illustrated.

As was noted in discussions concerning Fig. 8, present data showed a strong unit Reynolds number influence on transition above $\simeq 0.39 \times 10^6$/cm ($\simeq 10^6$/in.), but appeared to indicate a lessening influence as (U_e/ν_e) was decreased below $\simeq 0.39 \times 10^6$/cm ($\simeq 10^6$/in.). In his discussions of linear stability theory and its relationship to unit Reynolds number influence on transition, Reshotko[22] has postulated that, for a given disturbance environment, Re_{TR} is proportional to $(U_e/\nu_e)^n$, where the exponent n may be a function of M_e, $(T_w/T_{aw})_e$, and possibly even (U_e/ν_e) itself, to allow for deviations from a strict power-law dependence. Present data taken by themselves or when viewed in comparison with lower (U_e/ν_e) results of Stetson and Krogmann may provide an example of this postulated behavior, i.e., unit Reynolds number influence on transition depending on the unit Reynolds number regime experienced.

C. Transition Zone Asymmetry Results

Experimental information concerning the three-dimensional or asymmetric nature of transition on slender bodies at angle of attack is important for two reasons. First, as discussed in Sec. IV, a procedure must be available for correcting ballistics range ($\phi > 0$ deg, $\alpha > 0$ deg) transition data to zero angle of attack. As noted, Fig. 4 was used by Potter[10,11] and herein for this purpose. Such a family of curves by itself provides no insight as to why transition asymmetries develop at $(\alpha/\theta_c) > 0$; rather it provides an empirical description of these asymmetries at test conditions close to those of the two ballistics range experiments under discussion.

The second reason for providing a valid model for transition-zone asymmetry stems from design requirements to accurately predict asymmetric heat-transfer distributions, and asymmetric forces/moments (both shear and induced-pressure components), on slender free-flight bodies at angle of attack.

Comparisons of all transition run-length data measured during the present program were made with curves reported by Potter.[10,11] Results were plotted in terms of nondimensional transition run length $(X_{TR}/X_{TR,\alpha=0})$ vs circumferential body angle ϕ, from windward (0 deg) to leeward (180 deg), with (α/θ_c) as a parameter (see Fig. 22 of Ref. 12).

Since primary-ray X_{TR} values were corrected via linear interpolation between Potter's $\phi = 0$ deg and 60 deg curves in order to define $X_{TR,\alpha=0}$, agreement between present data and Potter's curves was "forced" for $\phi < 45$ deg. However, having defined $X_{TR,\alpha=0}$ for each station of each trajectory, it was then used to nondimensionalize measured X_{TR} values on the three nonprimary rays (45 deg $\leq \phi \leq$ 180 deg). No attempt was made to categorize data in terms of wall temperature ratio, unit Reynolds number, etc., consistent with the principal assumption behind Fig. 4, i.e., that transition zone asymmetry on sharp, slender cones is a function solely of (α/θ_c).

Several observations were made. First, at $\alpha \simeq 0$ deg, present data exhibited at $\pm 20\%$ axial variation about the nominal value of 1.0 for all circumferential locations. Such variations are a direct result of taking a finite number of "instantaneous" data samples of a basically unsteady (time-varying) flow phenomenon.[14] As angle of attack increased, transition was noted to move increasingly forward on the cone's leeward rays. Nonprimary-ray data ($\phi \geq 45$ deg) remained within an approximate $\pm$20-25% band about Potter's curves. Based on these comparisons alone, the assumption of transition zone asymmetry depending solely on (α/θ_c) appeared, to first order, to be justified.

Figures 10 and 11 show two comparisons of present data and Potter's curves with other Mach 5 transition zone asymmetry data: Krogmann,[28] Korsia and Marcillat,[30] Stetson and Rushton,[27] and Whitfield and Dougherty[29] (Fig. 11 only). Coordinates are those described above.

At a nondimensional angle of attack of $\simeq 0.4$ (Fig. 10) all data, save the windward-ray data of Krogmann, were noted to be self-consistent. At a nominal (α/θ_c) value of $\simeq 0.2$ (Fig. 11) fairly wide variations between the various data sets were observed.

Transition zone asymmetry on sharp, slender cones may not, in fact, be adequately described by a singular dependence on (α/θ_c). Flow parameters such as Mach number, wall temperature ratio, unit Reynolds number, etc., may influence observed asymmetries; other potential sources of influence which must be considered are the disturbance environments associated with the particular facility utilized and the measurement technique(s) incorporated. In any case, combined results of Figs. 10 and 11 raise a question concerning the sensitivity of conclusions reached in Secs. V. A and B and in Refs. 10 and 11 to the correction procedure for ($\phi > 0$ deg, $\alpha > 0$ deg) utilized.

A review of available data shows that Potter's windward-ray curve (faired through data of Ward[16]) represents the minimum observed rearward movement of transition with increasing (α/θ_c), while the windward-ray data of Krogmann[28] represent the maximum rearward movement observed. As noted, all ($\phi > 0$ deg, $\alpha > 0$ deg) corrections to present X_{TR} values were applied only to primary-ray data ($\phi < 45$ deg), via linear interpolation between the $\phi = 0$ deg and

SOURCE	SYM.	TECHNIQUE	FACILITY	θ_c	α/θ_c	M_∞	AT $\alpha = 0^0$: $\left(\frac{T_w}{T_{aw}}\right)_e$	AT $\alpha = 0^0$: $\frac{U_e}{\nu_e}, \frac{1}{cm}$	AT $\alpha = 0^0$: $\frac{U_e^2}{\nu_e}, \frac{1}{SEC.}$
REDA	●	DUAL-PLANE SPARK SHADOWGRAPH (5 STATIONS)	RANGE [4 SHOTS]	5.°	.35-.45	4.5	.22-.48	0.41-1.05 x 10^6	0.48-1.09 x 10^{11}
KROGMANN	▮	SURFACE HEAT TRANSFER RATES	LUDWIEG TUBE	5.°	.35-.45	5.0	—	0.18-0.32 x 10^6	—
KORSIA & MARCILLAT	◇	SINGLE-LINE OILFLOW ("LIMITING STREAMLINES")	TUNNEL	7.5°	.40	5.0	~1.0	0.25 x 10^6	0.22 x 10^{11}
STETSON & RUSHTON	□	SURFACE HEAT TRANSFER RATES.	SHOCK TUNNEL	8.°	.50	5.5	.24-.28	~0.08-0.20 x 10^6	~0.1-0.25 x 10^{11}

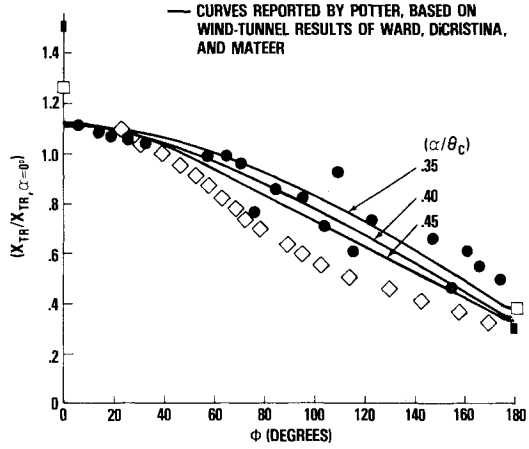

Fig. 10 Transition zone asymmetry—comparisons with other Mach 5 data, $0.35 \le (\alpha/\theta_c) \le 0.50$.

SOURCE	SYM.	TECHNIQUE	FACILITY	θ_c	α/θ_c	M_∞	AT $\alpha = 0^0$: $\left(\frac{T_w}{T_{aw}}\right)_e$	AT $\alpha = 0^0$: $\frac{U_e}{\nu_e}, \frac{1}{cm}$	AT $\alpha = 0^0$: $\frac{U_e^2}{\nu_e}, \frac{1}{SEC.}$
REDA	●	DUAL-PLANE SPARK SHADOWGRAPH (5 STATIONS)	RANGE [2 SHOTS]	5.°	.15-.20	4.5	.22-.35	0.35-0.98 x 10^6	0.43-1.53 x 10^{11}
KROGMANN	▮	SURFACE HEAT TRANSFER RATES	LUDWIEG TUBE	5.°	.15-.20	5.0	—	0.18-0.32 x 10^6	—
KORSIA & MARCILLAT	◇ ○	"LIMITING STREAMLINES" SCHLIEREN SURFACE PITOT	TUNNEL	7.5°	.20	5.0	~1.0	0.25 x 10^6	0.22 x 10^{11}
WHITFIELD & DOUGHERTY	▲	SURFACE PITOT	TUNNEL	5.°	.20	4.6	~1.0	—	—
STETSON & RUSHTON	▯	SURFACE HEAT TRANSFER RATES.	SHOCK TUNNEL	8.°	.25	5.5	.24-.28	~0.08-0.20 x 10^6	~0.1-0.25 x 10^{11}

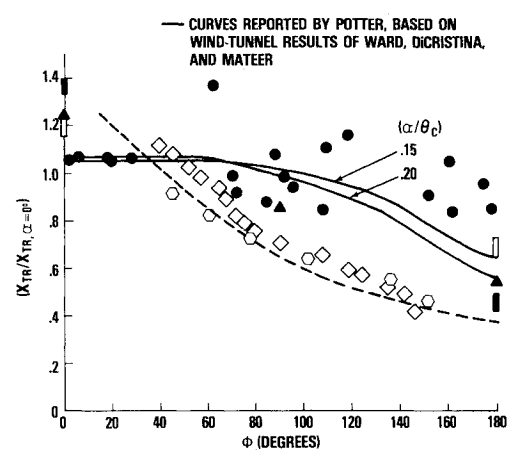

Fig. 11 Transition zone asymmetry—comparisons with other Mach 5 data, $0.15 \le (\alpha/\theta_c) \le 0.25$.

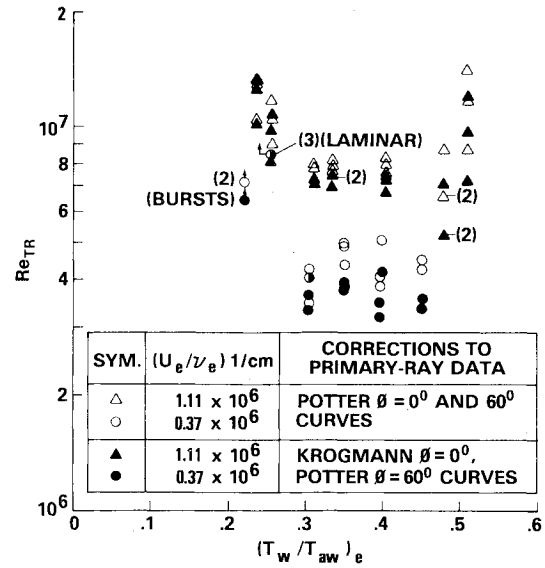

Fig. 12 Transition Reynolds number vs wall-to-adiabatic wall temperature ratio—sensitivity to corrections.

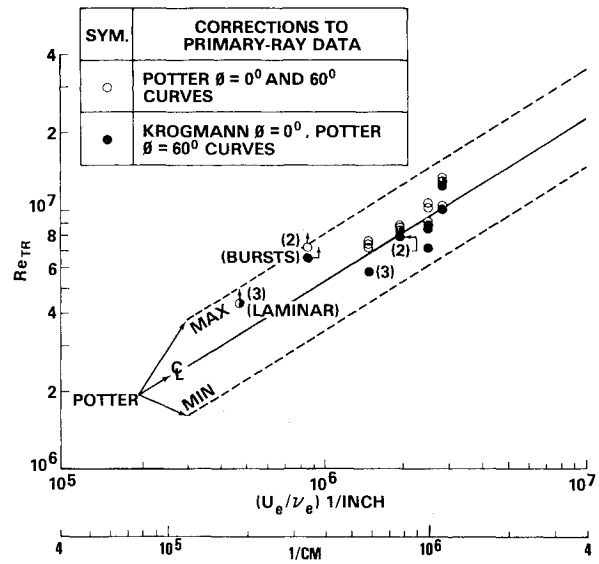

Fig. 13 Transition Reynolds number vs unit Reynolds number—sensitivity to corrections.

60 deg curves of Potter. It was decided to re-reduce these data, correcting for ($\phi > 0$ deg, $\alpha > 0$ deg) based on linear interpolation between Krogmann's $\phi = 0$ deg and Potter's $\phi = 60$ deg curves. Primary-ray data, corrected to $\alpha = 0$ deg by both techniques, are shown in Figs. 12 and 13.

Although absolute values for Re_{TR} were, for most flights, slightly reduced through use of Krogmann's curve, trends observed and conclusions reached in Secs. V. A and B, concerning wall-temperature-ratio and unit-Reynolds-number effects, remained unchanged.

Having addressed this sensitivity question, some final comments are offered concerning transition zone asymmetry on sharp, slender cones at angle of attack. If one reviews the individual data sets[16-18] averaged by Potter[10,11] to establish the family of curves shown in Fig. 4, significant variations similar to those witnessed in Fig. 11 become evident. (Fig. 18 of Ref. 10 shows a detailed comparison of these three data sets.) In particular, the hypersonic ($M_\infty = 10$) data of DiCristina[17] show a local maximum in $(X_{TR}/X_{TR,\alpha=0})$ near $\phi \simeq 90$ deg, while the lower Mach number data ($M_\infty \le 8$) of Mateer[18] show a monotonic decay in this parameter as ϕ

increases from 0 to 180 deg. The point is that, while it is generally accepted that transition moves rearward on the windward ray and forward on the leeward ray as angle of attack is increased, a complete understanding or description of the shape of the transition front between these extremes does not appear to be in hand.

VI. Conclusions

1) Transition reversals with increased wall cooling were observed at both unit Reynolds numbers tested. At 1.11×10^6/cm (2.82×10^6/in.), cooling was noted to be destabilizing in the regime $\simeq0.5\geq(T_w/T_{aw})_e\geq\simeq0.35$, and stabilizing for $\simeq0.35\geq(T_w/T_{aw})_e\geq0.23$. At 0.37×10^6/cm (0.94×10^6/in.), cooling in the regime $\simeq0.45\geq(T_w/T_{aw})_e\geq\simeq0.3$ yielded no discernable trends, whereas a definite stabilizing influence was evident for $\simeq0.3\geq(T_w/T_{aw})_e\geq\simeq0.22$.

2) Data obtained at $(U_e/\nu_e)>\simeq0.39\times10^6$/cm ($\simeq10^6$/in.) showed a strong unit Reynolds number influence on transition, consistent with results observed by Potter, while data obtained at $(U_e/\nu_e)<\simeq0.39\times10^6$/cm ($\simeq10^6$/in.) indicated a lessening influence of unit Reynolds number on transition.

3) Pairing of transition Reynolds numbers measured at 0.37 and 1.11×10^6/cm (0.94 and 2.82×10^6/in.) for each nominal wall temperature ratio tested, showed a unit Reynolds number influence on transition to exist over the entire $(T_w/T_{aw})_e$ regime tested.

4) Observed trends of transition Reynolds number with $(T_w/T_{aw})_e$ and (U_e/ν_e), as measured on the cone's most-windward ray, were found, via a sensitivity study, to be unaffected by the angle-of-attack correction procedure utilized.

5) Transition zone asymmetry data in the regime $0<(\alpha/\theta_c)\leq0.63$, as measured on the cone's three most-leeward rays, were found to be consistent with an empirical model reported by Potter. As angle of attack increased, leeward-ray transition locations were noted to move increasingly forward. However, comparisons of present data and Potter's curves with other Mach 5 data illustrated that transition zone asymmetry may not be adequately described by a singular dependence on (α/θ_c).

Acknowledgment

This research was jointly sponsored by Naval Air Systems Command, W.C. Volz, monitor, and Naval Sea Systems Command, L. Pasiuk, monitor.

References

[1] Pate, S.R. and Schueler, C.J., "Radiated Aerodynamic Noise Effects on Boundary-Layer Transition in Supersonic and Hypersonic Wind Tunnels," *AIAA Journal,* Vol. 7, March 1969, pp. 450-457.

[2] Dougherty Jr., N.S., "Correlation of Transition Reynolds Number with Aerodynamic Noise Levels in a Wind Tunnel at Mach Numbers 2.0-3.0," *AIAA Journal,* Vol. 13, Dec. 1975, pp. 1670-1671.

[3] Morkovin, M.V., "Instability, Transition to Turbulence and Predictability," AGARD-AG-236, July 1978.

[4] Morkovin, M.V., "Technical Evaluation Report of the Fluid Dynamics Panel Symposium on Laminar-Turbulent Transition," AGARD-AR-122, June 1978.

[5] Reshotko, E., "Boundary-Layer Stability and Transition," *Annual Review of Fluid Mechanics,* Vol. 8, 1976, pp. 311-349.

[6] Reshotko, E., "A Program for Transition Research," *AIAA Journal,* Vol. 13, March 1975, pp. 261-265.

[7] Sheetz Jr., N.W., "Ballistics Range Boundary-Layer Transition Measurements on Cones at Hypersonic Speeds," Symposium on Viscous Drag Reduction, LTV Research Center, Dallas, Texas, Sept. 1968, pp. 53-83, Plenum Press, New York, 1969.

[8] Sheetz Jr., N.W., "Ballistics Range Experiments on the Effect of Unit Reynolds Number on Boundary-Layer Transition," Eighth Navy Symposium on Aeroballistics, Naval Weapons Center/Corona Labs, Calif., May 1969.

[9] Potter, J.L., "Observations on the Influence of Ambient Pressure on Boundary-Layer Transition," *AIAA Journal,* Vol. 6, Oct. 1968, pp. 1907-1911.

[10] Potter, J.L., "The Unit Reynolds Number Effect on Boundary-Layer Transition," Ph.D. Thesis, Vanderbilt University, May 1974.

[11] Potter, J.L., "Boundary-Layer Transition on Supersonic Cones in an Aeroballistic Range," *AIAA Journal,* Vol. 13, March 1975, pp. 270-277.

[12] Reda, D.C., "Boundary-Layer Transition Experiments on Sharp, Slender Cones in Supersonic Freeflight," NSWC/WOL TR 77-59, Sept. 1977.

[13] Laderman, A.J., "Review of Wind-Tunnel Freestream Pressure Fluctuations," *AIAA Journal,* Vol. 15, April 1977, pp. 605-608.

[14] Potter, J.L. and Whitfield, J.D., "Effects of Slight Nose Bluntness and Roughness on Boundary-Layer Transition in Supersonic Flows," *Journal of Fluid Mechanics,* Vol. 12, No. 4, 1962, pp.501-535.

[15] Murphy, C.H., "Data Reduction for the Free Flight Spark Ranges," Ballistic Research Laboratories, Aberdeen Proving Ground, Md., BRL Rep. No. 900, Feb. 1954.

[16] Ward, L.K., "Influence of Boundary-Layer Transition on Dynamic Stability at Hypersonic Speeds," *Transactions of 2nd Technical Workshop on Dynamic Stability Testing,* Vol. II, Arnold Engineering Development Center, 1965.

[17] DiCristina, V., "Three-Dimensional Laminar Boundary-Layer Transition on a Sharp 8° Cone at Mach 10," *AIAA Journal,* Vol. 8, May 1970, pp. 852-856.

[18] Mateer, G.G., "Effects of Wall Cooling and Angle of Attack on Boundary Layer Transition on Sharp Cones at $M_\infty=7.4$," NASA TN D-6908, 1972.

[19] Lees, L. and Reshotko, E., "Stability of the Compressible Laminar Boundary Layer," *Journal of Fluid Mechanics,* Vol. 12, 1962, pp. 555-590.

[20] Reshotko, E., "Transition Reversal and Tollmien-Schlichting Instability," *The Physics of Fluids,* Vol. 6, March 1963, pp. 335-342.

[21] Mack, L.M., "The Stability of the Compressible Laminar Boundary Layer According to a Direct Numerical Solution," AGARDograph 97, 1965, pp. 483-501.

[22] Reshotko, E., "Stability Theory as a Guide to the Evaluation of Transition Data," *AIAA Journal,* Vol. 7, June 1969, pp. 1086-1091.

[23] Richards, B.E. and Stollery, J.L., "Further Experiments on Transition Reversal at Hypersonic Speeds," *AIAA Journal,* Vol. 4, Dec. 1966, pp. 2224-2226.

[24] Kendall, J.M., "Wind-Tunnel Experiments Relating to Supersonic and Hypersonic Boundary-Layer Transition," *AIAA Journal,* Vol. 13, March 1975, pp. 290-299.

[25] Mack, L.M., "Linear Stability Theory and the Problem of Supersonic Boundary-Layer Transition," *AIAA Journal,* Vol. 13, March 1975, pp. 278-289.

[26] Boison, J.C., "Investigation of Test Facility Environmental Factors Affecting Boundary-Layer Transition," AFFDL-TR-73-106, Sept. 1973.

[27] Stetson, K.F., and Rushton, G.H., "Shock Tunnel Investigation of Boundary-Layer Transition at M=5.5," *AIAA Journal,* Vol. 5, May 1967, pp. 899-906.

[28] Krogmann, P., "An Experimental Study of Boundary-Layer Transition on a Slender Cone at Mach 5," AGARD-CP-224, Symposium on Laminar-Turbulent Transition, Technical University of Denmark, Copenhagen, Denmark, May 1977.

[29] Whitfield, J.D. and Dougherty Jr., N.S., "A Survey of Transition Research at AEDC," AGARD-CP-224, Symposium on Laminar-Turbulent Transition, Technical University of Denmark, Copenhagen, Denmark, May 1977; also published as AEDC-TR-77-52, July 1977.

[30] Korsia, A. and Marcillat, J.F., "Three-Dimensional Boundary-Layer Transition on a Yawed 7.5° Sharp Cone at M=5," AGARD-CP-224, Symposium on Laminar-Turbulent Transition, Technical University of Denmark, Copenhagen, Denmark, May 1977.